

Nanoscale

rsc.li/nanoscale



ISSN 2040-3372

















PAPER

Xiaoxuan Liu, Ling Peng *et al.*
Bola-amphiphilic glycodendrimers for targeting glial cells in
the brain



Cite this: *Nanoscale*, 2025, **17**, 27869

Bola-amphiphilic glycodendrimers for targeting glial cells in the brain

Zhancun Bian, ^{a,b} Wenzheng Zhang, ^{b,c} Stefano Garofalo, ^d Dinesh Dhumal, ^b Junyue Zheng, ^a Tom Roussel, ^b Erik Laurini, ^e Christina Galanakou, ^b Clotilde Lauro, ^d Marc Maresca, ^e Yi Xia, ^c Dandan Zhu, ^a Sabrina Pricl, ^{f,g} Xiaoxuan Liu, ^{*a} Cristina Limatola ^{d,h} and Ling Peng ^{*b}

Targeting glial cells in the brain constitutes a formidable challenge due to the presence of the blood–brain barrier (BBB) and the difficulty in achieving specific targeting. Intranasal (IN) administration offers a promising solution to bypass the BBB for delivery directly to the brain, while nanotechnology-based delivery provides tailored targeting capabilities. Here, we report dendrimer-based nanosystems developed for IN administration to target astrocytes and microglia, two types of glial cells that play important roles in maintaining brain homeostasis. Specifically, we demonstrate that bola-amphiphilic glycodendrimers, **1a** and **1b**, which bear glucose and mannose terminals, respectively, target astrocytes and microglia in the mouse brain. These two glycodendrimers, composed of a hydrophobic bola-lipid in the middle connected with two hydrophilic poly(amidoamine) dendrons, were effectively synthesized *via* a click reaction using unprotected carbohydrate building units, and self-assembled into small and spherical nanoparticles by virtue of their amphiphilicity. In a mouse model, both dendrimer nanoparticles successfully reached the brain following IN administration, where the glucose-dendrimer **1a** selectively targeted astrocytes and the mannose-dendrimer **1b** targeted microglia. These findings highlight the potential of glycodendrimer-based nanosystems for precise targeting in the brain and offer a promising perspective for treating central nervous system (CNS) diseases.

Received 17th July 2025,
Accepted 24th October 2025

DOI: 10.1039/d5nr03017j

rsc.li/nanoscale

Introduction

Central nervous system (CNS) diseases pose significant therapeutic challenges due to the presence of the blood–brain

barrier (BBB), the complexity of brain pathologies and the difficulty of delivering drugs effectively to the desired glial cells in specific brain regions.^{1,2} Astrocytes and microglia are two types of glial cells that play important roles in maintaining brain homeostasis, and many CNS disorders are closely linked to the dysfunction of these glial cells.^{3,4} Specifically, astrocytes support neuronal function, regulate synaptic activity, and maintain the integrity of the BBB,^{5–7} while microglia serve as the brain's primary immune cells, orchestrating inflammatory responses and tissue repair.^{4,8} Targeting astrocytes and microglia or modulating their activity presents a promising therapeutic approach, but remains a major challenge due to the restrictive nature of the BBB and the lack of cell-specific targeting strategies.^{8–11}

Intranasal (IN) administration has emerged as a non-invasive and efficient strategy to bypass the BBB by delivering therapeutics directly to the brain *via* the olfactory and trigeminal nerve pathways.¹² This approach avoids systemic circulation, enhances CNS targeting, and minimizes peripheral side effects, making it particularly attractive for tackling CNS disorders.¹³ To further improve the efficiency and specificity of IN delivery, nanotechnology-based drug delivery systems have

^aState Key Laboratory of Natural Medicines, Joint International Research Laboratory of Target Discovery and New Drug Innovation (Ministry of Education), Jiangsu Key Laboratory of Drug Discovery for Metabolic Diseases, Center of Advanced Pharmaceuticals and Biomaterials, China Pharmaceutical University, Nanjing, P. R. China. E-mail: xiaoxuanliu@cpu.edu.cn

^bAix Marseille University, CNRS, Center Interdisciplinaire de Nanoscience de Marseille, UMR 7325, “Equipe Labellisée Ligue Contre le Cancer”, Marseille, France. E-mail: ling.peng@univ-amu.fr

^cChongqing Key Laboratory of Natural Product Synthesis and Drug Research, Innovative Drug Research Center, School of Pharmaceutical Sciences, Chongqing University, Chongqing, P. R. China

^dDepartment of Physiology and Pharmacology, Sapienza University of Rome, Rome, Italy

^eAix Marseille Univ, CNRS, Centrale Med, ISM2, 13013 Marseille, France

^fMolecular Biology and Nanotechnology Laboratory (MoBNL@UnitS), DEA, University of Trieste, 34127 Trieste, Italy

^gDepartment of General Biophysics, Faculty of Biology and Environmental Protection, University of Lodz, 90-236 Lodz, Poland

^hIRCCS Neuromed, Pozzilli, Italy



been developed for administration *via* the IN route.^{14–16} Nanoparticulate drug formulations have been shown to improve drug stability, prolong drug residence time in the nasal cavity and enhance drug penetration across the nasal mucosa.¹⁴ Most importantly, nanoparticles decorated with targeting ligands have enabled precise targeting and drug delivery to specific regions and cells in the brain, further improving therapeutic outcomes.^{14–16} For example, insulin-functionalized nanoparticles leverage insulin receptor overexpression in hippocampal neurons to achieve region-specific targeting and delivery of protein drugs, raising therapeutic efficacy for neurodegenerative diseases.¹⁷ Also, nanoparticles functionalized with glucose or mannose units have been investigated to enhance specific delivery and targeting respectively to astrocytes *via* glucose transporter 1 (GLUT1)^{18,19} or activated microglia *via* mannose receptors.^{20,21} Such specific targeting using nanotechnology-based drug delivery thus provides new therapeutic options for treating CNS disorders.

Dendrimers are a special class of precision nanomaterials that are highly valuable for nanotechnology-based delivery to the CNS by virtue of their unique well-defined dendritic struc-

ture and cooperative multivalency confined within a nanoscale 3D architecture.^{22–24} In particular, amphiphilic dendrimers, composed of distinct hydrophobic and hydrophilic entities, are able to self-organize into nano-assemblies^{25–27} capable of encapsulating and delivering various pharmaceutical agents, including anticancer drugs,^{28–30} nucleic acid therapeutics^{31,32} and bioimaging agents.^{33–35} Specifically, bola-amphiphilic dendrimers consist of two hydrophilic dendrons connected by a hydrophobic “bola-lipid” core scaffold.^{31,36–38} This design was inspired by the bola-amphiphiles found in extremophile archaea, which possess a unique bola-lipid monolayer membrane structure and exhibit robust tolerance to extreme conditions such as high temperature, acidity, salinity, *etc.*³⁹ All these features have been successfully harnessed for robust and efficient drug delivery.^{31,36–38}

We have recently developed bola-amphiphilic glycodendrimers **Ia** and **Ib** (Fig. 1A) functionalized with glucose and mannose terminals to target astrocytes and microglia, respectively.⁴⁰ The multiple carbohydrate units on the dendrimer surface enhance binding affinity and selectivity through the multivalent cooperative glycoside cluster effect, a mechanism

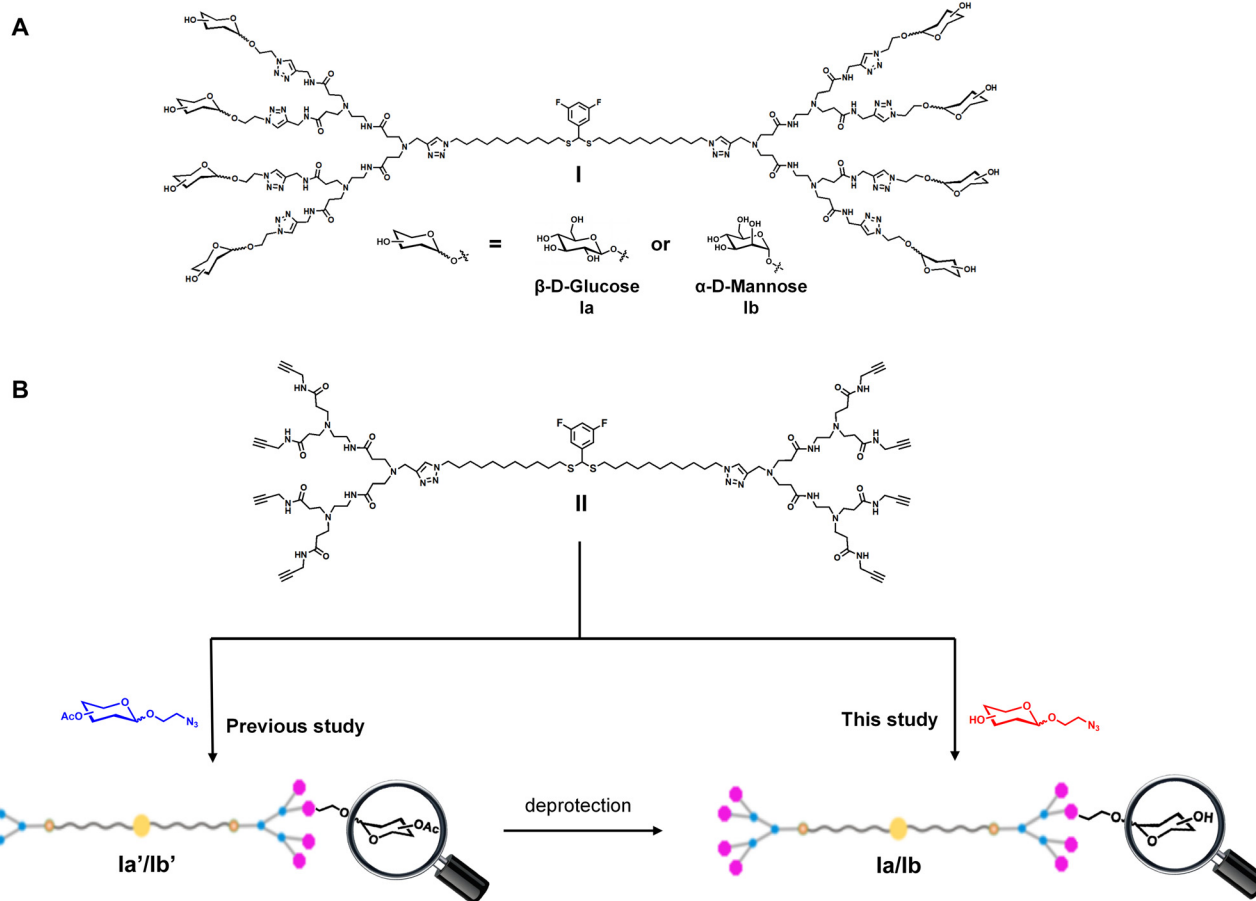


Fig. 1 (A) Bola-amphiphilic glycodendrimers, **Ia** and **Ib**, bearing glucose- and mannose-terminals for specifically targeting astrocytes and microglia, respectively, in the brain. (B) Synthetic strategies for the bola-amphiphilic dendrimers **Ia** and **Ib** using protected carbohydrate building units in a previous study (left) and unprotected carbohydrate units in this study (right).



observed in the interaction between glycans and glycoproteins in nature.^{41,42} Additionally, the “bola-lipid” chain in **Ia** and **Ib** is shorter than the membrane bilayer, preventing their potential anchoring to the cell membrane. Here, we extended these findings to an *in vivo* mouse model to evaluate the ability of these two glycodendrimers to reach and selectively target glial cells following IN administration.

Notably, we also introduced an optimized synthetic route for **Ia** and **Ib** to enhance efficiency and yield. Our previous method involved using protected carbohydrates that carry azido functionalities for conjugation with the alkynyl-bearing dendrimer **II** *via* a click reaction (Fig. 1B, left). The resulting dendrimers required a tedious and challenging purification process, along with the subsequent removal of the protecting groups. This made the synthesis particularly time-consuming and labor-intensive, as well as compromised product yield. To overcome these drawbacks, we elaborated a new and more efficient synthesis route using unprotected carbohydrate units, which significantly simplified the purification procedure and improved overall yields (Fig. 1B, right). We present herein a novel synthetic approach for preparing the bola-amphiphilic glycodendrimers **Ia** and **Ib** and demonstrate their effective targeting of astrocytes and microglia, respectively, in the mouse brain following IN administration. This study highlights the promise of glycodendrimers as tools for the precision targeting of glial cells, offering a novel strategy to modulate glial cell activity for treating CNS disorders.

Results and discussion

Reliable and simplified synthesis of glycodendrimers

The synthesis of both **Ia** and **Ib** started with the alkyne-terminated dendrimer **II**, the precursor for click chemistry conjugation (Fig. 1B). We previously prepared **II** by condensing the carboxylic acid-terminated dendrimer **III** with propargylamine in DMF using EDCI and HOBt, along with molecular sieves as a drying agent (Fig. 2).⁴⁰ However, that approach produced inconsistent yields, ranging from 0 to 81%. To address this issue, we added DIPEA as an auxiliary base to activate the carboxylic acid terminals for reaction with EDCI, while also neutralizing the generated hydrogen chloride to promote the reaction. To further optimize the process, we replaced the high-boiling-point solvent DMF with THF as the solvent, thereby avoiding the time-intensive preparation of anhydrous DMF and its removal during work-up. Collectively, these adjustments rendered the coupling reaction particularly efficient, consistently affording the alkyne-terminated dendrimer **II** in stable yields exceeding 75% even without the use of molecular sieves. This greatly simplified the synthesis and purification processes.

We then conjugated the alkyne-terminated dendrimer **II** with unprotected carbohydrate derivatives bearing azido groups *via* click chemistry to obtain glycodendrimers **Ia** and **Ib**, respectively (Fig. 2). The click reaction between **II** and **a** proceeded efficiently in the presence of CuSO₄·5H₂O and sodium

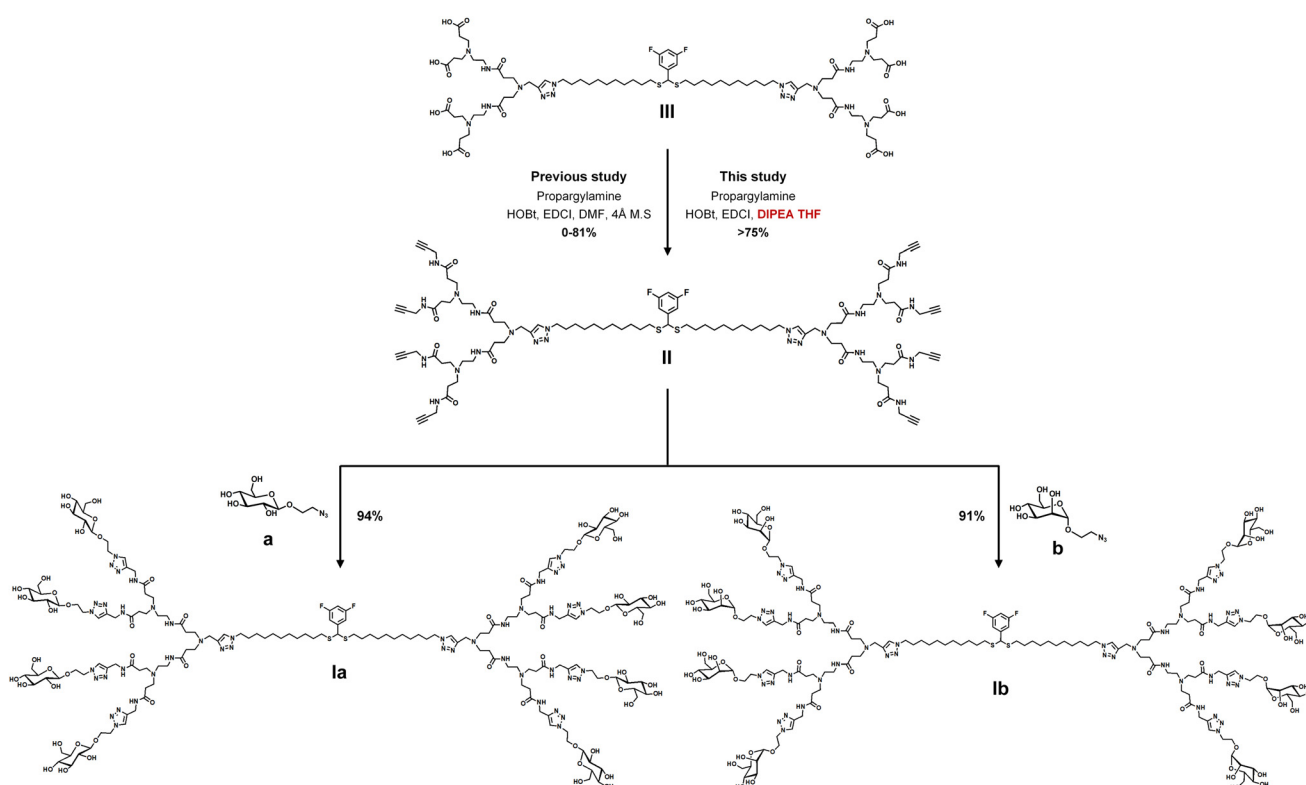


Fig. 2 Synthetic methods for the alkyne-terminated bola-amphiphilic dendrimer (**II**) and bola-amphiphilic glycodendrimers **Ia** and **Ib**.



ascorbate, despite challenges associated with multi-site reactions and steric hindrance of multiple glucose units at the terminals. In addition, **Ia** was easily and conveniently isolated and purified by employing Chelex® resin to chelate and remove the copper ions, followed by dialysis and Sephadex chromatography to eliminate other impurities from the crude product. Subsequent lyophilization gave the final dendrimer **Ia** as a white solid with an excellent yield exceeding 94%.

Compared to the previous method using the protected glucose derivative **a'** (Fig. 3, right), the new approach with the unprotected glucose derivative **a** (Fig. 2, left and Fig. 3, left) not only reduced the synthesis time and simplified the purification process but also achieved higher yields. Using the same strategy, we also successfully prepared the mannose-dendrimer **Ib** as a white solid with an outstanding yield of 91% (Fig. 2, right). The structural integrity and purity of all synthesized dendrimers were confirmed using ^1H -, ^{13}C -, and ^{19}F -NMR spectral analyses, as well as high-resolution mass spectrometry (HRMS) (Fig. S1–S3).

Self-assembly of glycodendrimers into small, uniform and stable nanoparticles

With the synthesized dendrimers **Ia** and **Ib** in hand, we further studied their self-assembly into nanoparticles in water. Owing to their amphiphilicity, both **Ia** and **Ib** spontaneously formed small nanoparticles (termed **Ia@** and **Ib@**, respectively) in water, as demonstrated by dynamic light scattering (DLS) analysis (Fig. 4A and B). Further transmission electron microscopy (TEM) images of **Ia@** and **Ib@** (Fig. 4C and D) confirmed the presence of small, uniform, spherical particles measuring 25 ± 3 nm for **Ia@** and 20 ± 3 nm for **Ib@**, respectively, consistent with the typical characteristics of nanomicelles. In addition,

fluorescence spectral analysis revealed similar critical micelle concentrations (CMC) of $34 \mu\text{M}$ for **Ia@** and $30 \mu\text{M}$ for **Ib@** (Fig. 4E and F). It is also worth noting that both **Ia@** and **Ib@** have slightly positive zeta potentials, +12 mV and +11 mV, respectively (Fig. 4G and H), which can help prevent nanoparticle aggregation and may also contribute to minimizing potential toxicity arising from possible interactions with serum proteins or cell membranes, thereby supporting their favorable safety profile reported previously.⁴⁰

We next employed isothermal titration calorimetry (ITC) to elucidate the thermodynamic parameters governing the self-assembly and micellization of dendrimers **Ia** and **Ib** following a well-validated procedure.^{33,43} The demicellization thermograms for both dendrimers exhibited comparable profiles, indicating similar micellization behaviors (Fig. 4I and J). For **Ia**, the CMC was determined to be $21 \mu\text{M}$, while **Ib** exhibited a slightly lower CMC of $16 \mu\text{M}$. These values are consistent with the data obtained from the fluorescence assay. The standard Gibbs free energy of micellization (ΔG_{mic}) was calculated using the following relationship:

$$\Delta G_{\text{mic}} = RT \ln(\text{CMC}')$$

where R is the universal gas constant ($1.987 \text{ cal mol}^{-1} \text{ K}^{-1}$), T is the absolute temperature in kelvin and CMC' is the critical micellization concentration expressed in molar units. The calculated ΔG_{mic} values were $-8.78 \text{ kcal mol}^{-1}$ for **Ia@** and $-8.96 \text{ kcal mol}^{-1}$ for **Ib@**, indicating a spontaneous micellization process for both bola-amphiphilic dendrimers. The enthalpy change of micellization (ΔH_{mic}) was obtained directly from the ITC measurements, yielding values of $-5.31 \text{ kcal mol}^{-1}$ for **Ia@** and $-4.90 \text{ kcal mol}^{-1}$ for **Ib@**, indicative of an exothermic process. The entropy change ($T\Delta S_{\text{mic}}$) associated

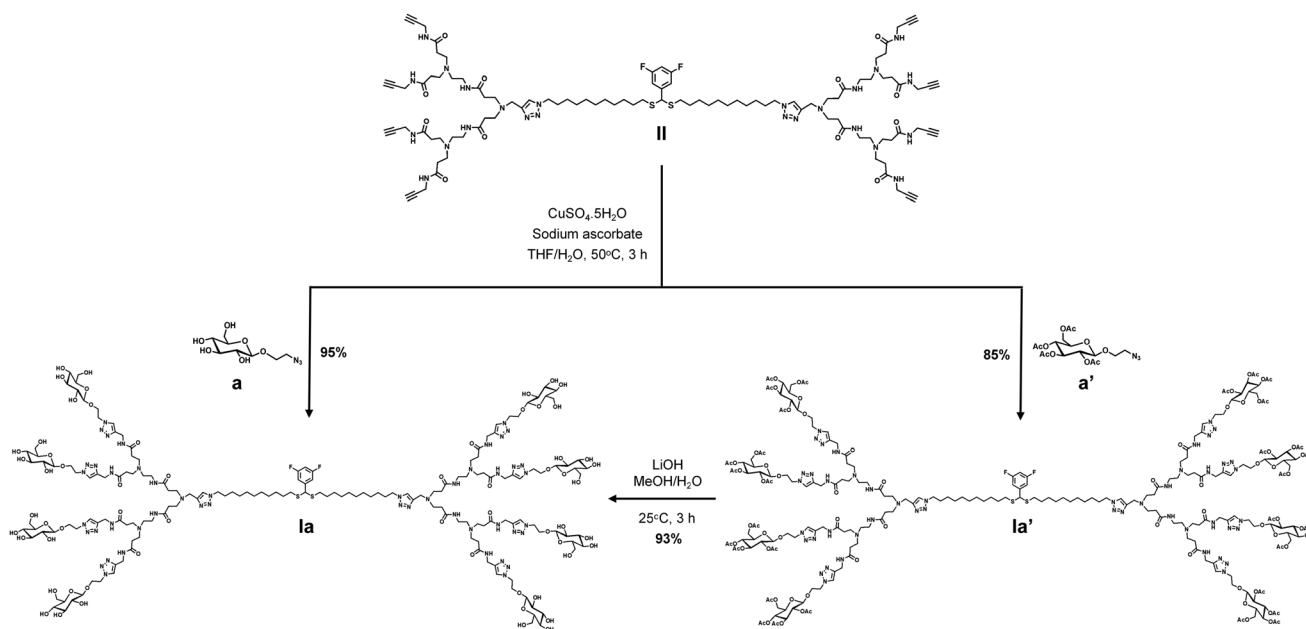


Fig. 3 Synthesis of the bola-amphiphilic glucose-dendrimer (**Ia**) using an unprotected carbohydrate derivative (left) and a protected carbohydrate unit (right).





Fig. 4 Self-assembly of the bola-amphiphilic glycodendrimers **1a** and **1b** into small and uniform nanoparticles, **1a@** and **1b@**, respectively. Dynamic light scattering (DLS) analysis of nanoparticles (A) **1a@** and (B) **1b@**, respectively, showing their size and size distribution; transmission electron microscopy (TEM) images of (C) **1a@** and (D) **1b@** (scale bar: 100 nm), demonstrating their uniform small nanoparticle morphology; critical micelle concentration measured using fluorescence spectral analysis with Nile red for (E) **1a@** and (F) **1b@**, respectively. Zeta-potential analysis of (G) **1a@** and (H) **1b@**, respectively. Representative ITC profiles for the demicellization process of (I) **1a@** and (J) **1b@** in water. The dotted lines represent the data fitting with a sigmoidal function, and the insets display the corresponding ITC raw thermograms. Zoomed snapshots from the equilibrated MD trajectory of (K) **1a@** and (L) **1b@**.



with micellization was derived from the Gibbs–Helmholtz equation:

$$T\Delta S_{\text{mic}} = \Delta H_{\text{mic}} - \Delta G_{\text{mic}}.$$

Consequently, the $T\Delta S_{\text{mic}}$ values were calculated to be 3.47 kcal mol⁻¹ for **Ia@** and 4.06 kcal mol⁻¹ for **Ib@**, indicative of an increase in system entropy upon micellization. This characteristic is due to the release of structured water molecules from the hydration shells of the hydrophobic tails as the dendrimers aggregate into micelles. Such thermodynamic parameters suggest a combined enthalpic- and entropic-driven micellization. The enthalpy change, arising from favorable interactions between the hydrophilic head groups and the solvent, as well as cooperative packing within the poly(amido-amine) dendrons, plays a key role in micelle stabilization. Simultaneously, the positive entropy values support the notion of increasing disorder associated with water molecule displacement, rendering the system thermodynamically favorable. This combination of enthalpic and entropic factors underscores the efficient self-assembly of both dendrimers into stable micellar structures. In summary, ITC analysis demonstrated that both glucose and mannose dendrimers undergo spontaneous, exothermic micellization with comparable thermodynamic parameters and mechanisms driven by a combination of enthalpic stabilization and entropic favorability.

We also examined the nanomicellar formation of both dendrimers using atomistic molecular dynamics (MD) simulations by employing a robust computational protocol.^{44–46} Starting from a randomized distribution of 22 molecules in solution, the MD simulations resulted in stable micellar nanoassemblies, as depicted in Fig. 4K and L. The average micelle gyration radii (R_g) were determined to be approximately 6.8 ± 0.3 nm for **Ia@** and 6.6 ± 0.2 nm for **Ib@** (Fig. S4, in the SI), demonstrating high consistency between the two systems and aligning well with the data obtained with the experimental techniques DLS and TEM. The similarity in R_g values suggests that both micelles achieve comparable structural stability and compaction in aqueous environments. A detailed conformational analysis of the micellar architectures, coupled with radial distribution function (RDF) analysis, revealed the spatial organization of the terminal carbohydrate moieties and the hydrophobic core components (Fig. S4, in the SI). Both **Ia@** and **Ib@** feature terminal carbohydrate residues that are predominantly exposed on the micellar surface. This structural arrangement ensures their accessibility and the ability to interact effectively with biological targets. The presentation of glucose or mannose residues at the micellar periphery supports their potential recognition by specific biomolecular counterparts, reinforcing their potential functional roles in targeted interactions. Moreover, the same RDF analysis revealed that the hydrophobic regions of both micelles remain primarily concentrated toward the micellar core, effectively shielded from the solvent, as shown by the corresponding RDFs. Despite minor differences in the orientation of the terminal moieties, the micellar structures of **Ia@** and **Ib@** remain highly comparable, achieving an optimal surface presentation

of their functional groups, which is critical for their respective biological interactions. In short, ITC and MD simulations together confirm that both systems exhibit robust self-assembly behavior and form stable micellar architectures in solution.

Favorable safety profile and biocompatibility

For delivery to the brain *via* IN administration, the safety of nanoparticles is an important consideration. As we already assessed the cytotoxicity of **Ia@** and **Ib@** to human embryonic kidney cells (HEK293), mouse fibroblast cells (L929), and Madin–Darby canine kidney cells (MDCK) in our previous study,⁴⁰ we therefore focused, in this investigation, on evaluating their cytotoxicity to primary human nasal epithelial cells (hNEpCs), microglial BV2 cells, astrocyte C8-D1A cells, mouse brain endothelial bEnd.3 cells and neurons derived from N2a cells using the MTT assay (Fig. 5A). Both **Ia@** and **Ib@** showed no significant cytotoxicity to all tested cells, even at concentrations up to 100 μ M, highlighting excellent *in vitro* biocompatibility.

We further assessed the safety profiles of **Ia@** and **Ib@** in healthy mice upon intranasal administration, through analysis of inflammatory responses, blood biochemistry, and histopathological changes in major organs. As shown in Fig. 5B, no inflammation was observed in healthy mice following treatment with **Ia@** and **Ib@**, compared to the negative control group treated with PBS buffer. In contrast, mice administered with lipopolysaccharide (LPS) as a positive control exhibited markedly elevated levels of proinflammatory cytokines IL-1 β , IL-6, TNF- α , and IFN- γ . Moreover, the kidney function-related parameters (urea and creatinine), liver enzymes (alanine aminotransferase (ALT) and aspartate aminotransferase (AST)), and blood lipid parameters (triacylglycerol (TG) and total cholesterol (TCHO)) remained within normal ranges following intranasal administration of **Ia@** and **Ib@** (Fig. 5C), indicating the absence of hepatotoxicity or nephrotoxicity. Also, histological analysis using hematoxylin and eosin (H&E) staining revealed a normal tissue architecture and cellular morphology in the major organs of mice treated with **Ia@** and **Ib@**, suggesting no discernible pathological abnormalities compared to the PBS-treated control group (Fig. 5D). Collectively, these findings indicate that both **Ia@** and **Ib@** exhibit a favorable safety profile, highlighting their potential as candidates for subsequent *in vivo* studies targeting astrocytes and microglia in the brain.

Effective uptake in the brain and specific targeting of glial cells

As we already demonstrated that **Ia** and **Ib** target primary cell cultures of astrocytes and microglia, respectively, in our previous *in vitro* study,⁴⁰ we concentrated, in this investigation, on the examination of these two dendrimers to reach the brain and to specifically target astrocytes and microglia in animals using a healthy mouse as the animal model.

To facilitate the tracking of brain targeting and uptake, we loaded the nanomicelles **Ia@** and **Ib@** formed by the two dendrimers with the fluorescent dye Cy3, hereafter referred to as





Fig. 5 Safety evaluation of Ia@ and Ib@. (A) *In vitro* toxicity evaluation of Ia@ and Ib@ to primary human nasal epithelial cells (hNEpCs), microglial BV2 cells, astrocyte C8-D1A cells, mouse brain endothelial bEnd.3 cells and neurons derived from N2a cells in a dendrimer concentration range of 0 to 100 μM at 24 h post-treatment using the MTT assay. (B, C and D) *In vivo* toxicity evaluation of Ia@ and Ib@ in healthy mice ($n = 3$ for each group of mice). (B) Quantification of the major inflammatory cytokines in serum IL-1 β , IL-6, TNF- α , and INF- γ . (C) Liver and kidney function as well as blood lipid by quantifying the levels of biomarkers ALT, AST, UREA, CREA, TCHO and TG in serum. * $p \leq 0.001$, *** $p \leq 0.001$; significance was determined using one-way ANOVA (mean \pm SD, $n = 3$). (D) Histological analysis of tissues from major organs. Mice were intranasally administered with PBS, Ia@ and Ib@. Scale bar: 100 μm .

Cy3/Ia@ and Cy3/Ib@, respectively. Notably, both Cy3/Ia@ and Cy3/Ib@ showed similar size and surface charges to their corresponding non-labelled counterparts Ia@ and Ib@ (Fig. S5

in the SI), highlighting their relevance to mimic Ia@ and Ib@ for use in studying uptake into the brain as well as specific targeting towards astrocytes and microglia.



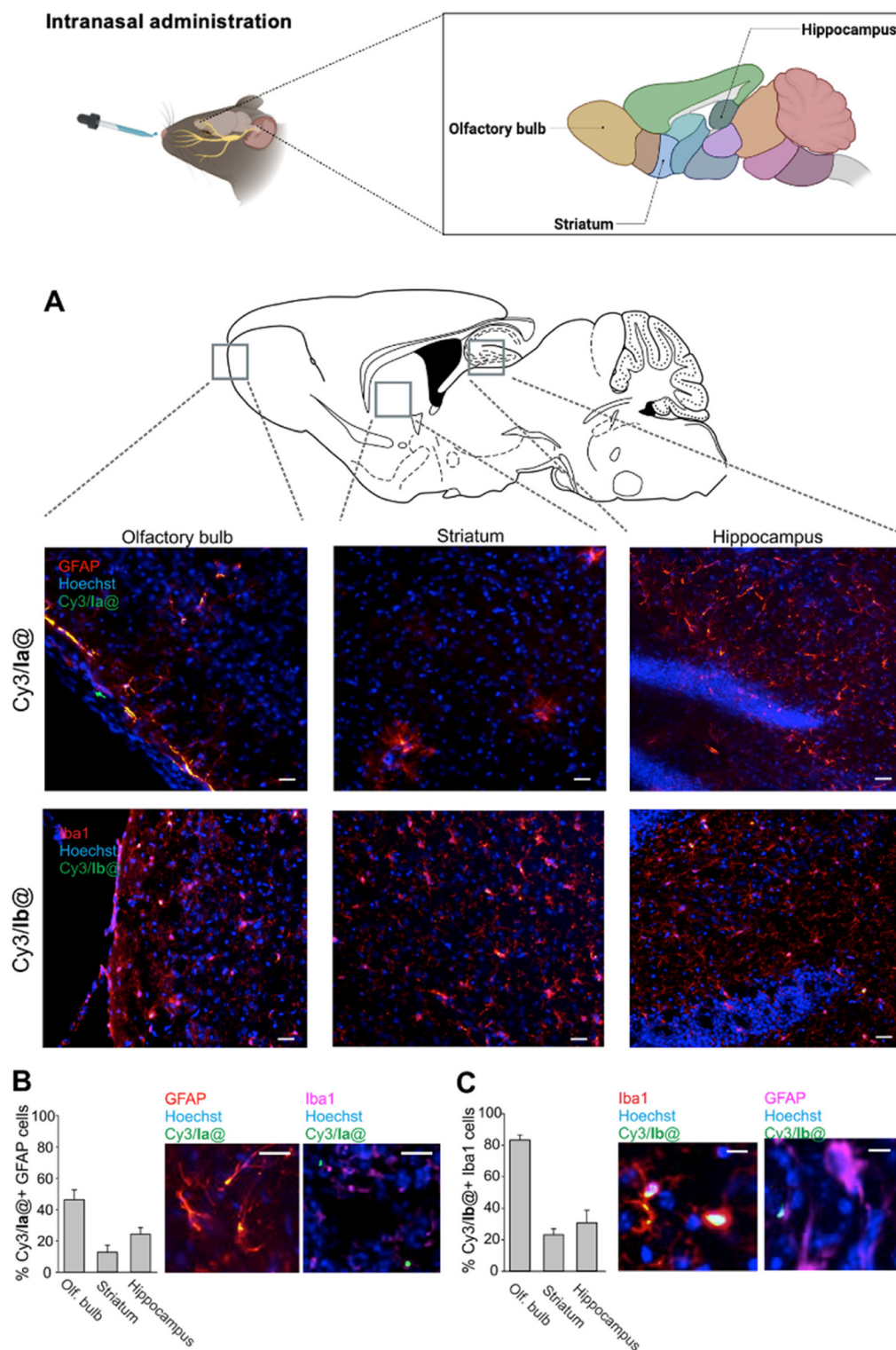


Fig. 6 Intranasally administered dendrimer nanoparticles reached the mouse brain. (A) Representative immunofluorescence images showing the astrocyte marker Glial Fibrillary Acidic Protein (GFAP; red) and Cy3/Ia@ (green) (upper panel), and the microglial marker ionized calcium binding adaptor molecule 1 (Iba1; red) and Cy3/Ib@ (green) (lower panel), with Hoechst (blue) to label nuclei, in the transversal section of the C57BL/6 mouse brain 24 h after intranasal administration of Cy3/Ia@ and Cy3/Ib@, respectively. Scale bar: 100 μ m. (B) Percentage of Cy3/Ia@+ GFAP cells in the olfactory bulb, striatum and hippocampus 24 h after intranasal administration of Cy3/Ia@ ($n = 5$ mice). Right: Representative immunofluorescence of GFAP (red) or Iba1 (cyan) and Cy3/Ia@ (green) in the brain of C57BL/6 mice (scale bar: 40 μ m). (C) Percentage of Cy3/Ib@+ Iba1 cells (red) in the olfactory bulb, striatum and hippocampus 24 h after intranasal administration of Cy3/Ib@ ($n = 5$ mice). Right: Representative immunofluorescence of Iba1 (red) or GFAP cells (cyan) and Cy3/Ib@ (green) in the brain of C57BL/6 mice (scale bar: 20 μ m). The mouse image was created with BioRender.



We then administered Cy3/**Ia**@ and Cy3/**Ib**@, respectively, to C57BL/6 mice *via* the IN route to track uptake into the mouse brain (Fig. 6). Fluorescence signals from Cy3 were observed in the olfactory bulb, hippocampus and striatum of the mice treated with either Cy3/**Ia**@ or Cy3/**Ib**@. It is worth mentioning that the olfactory bulb showed the highest number of fluorescent cells. This can be easily understandable as the olfactory bulb is the first part of the brain to encounter the agent when using IN administration (Fig. 6A).

Further immunohistochemistry analysis revealed co-localization of Cy3/**Ia**@ with astrocytes (Fig. 6B) and Cy3/**Ib**@ with microglia (Fig. 6C). No co-localization of Cy3/**Ia**@ with microglia (Fig. 6B) or Cy3/**Ib**@ with astrocytes (Fig. 6C) was observed. These findings demonstrate the effective and specific targeting of astrocytes by Cy3/**Ia**@ and microglia by Cy3/**Ib**@ within the mouse brain following IN administration. It is noted that single cell analyses revealed a macrophage-specific expression of the mannose receptor, with minor expression in a subset of immature microglia.^{47,48} Therefore, the Iba1+ cells co-labeled with Cy3/**Ib**@ might also result from the phagocytic activity of microglial cells and/or perivascular macrophage labeling.

Conclusion

In this study, we successfully prepared bola-amphiphilic glycodendrimers bearing glucose and mannose terminals using a simplified synthetic route and evaluated their ability to target specific glial cells in the brain *via* IN administration in a mouse model. The novel synthetic strategy, employing unprotected carbohydrate derivatives, provides a more efficient and reliable method for synthesizing glycodendrimers. This new approach reduces the number of synthesis steps and purification procedures while maintaining the structural integrity and purity, as well as achieving higher yields. Further biological evaluation demonstrated that both the glucose dendrimer **Ia** and the mannose dendrimer **Ib** exhibited excellent brain targeting ability, with **Ia** specifically homing in on astrocytes and **Ib** on microglia. Given the emerging therapeutic potential of modulating glial cell activity for treating neurological disorders, glycodendrimers **Ia** and **Ib** therefore hold great promise for translation into drug delivery systems to treat CNS diseases *via* the simple and non-invasive IN route. Our ongoing research is focused on advancing further along this promising avenue.

Author contributions

LP conceived and coordinated the project; LP, CL, and XL supervised the studies; ZB, WZ, DD, and TR performed synthesis and characterization; EL and SP performed ITC and computer modeling; SG, CL, CG, MM, and JZ performed the biological evaluation; ZB, WZ, JZ, DZ, DD, TR, SG, CL, CL, and LP analyzed the data; ZB, WZ, JZ, DZ, XL, EL, SG, CL, and LP wrote the manuscript; and all authors read and proofed the manuscript.

Conflicts of interest

The authors declare no competing interests.

Ethical statement

For intranasal administration, all animal procedures described in the present work were performed in accordance with the guidelines on the ethical use of animals from the European Community Council Directive of September 22, 2010 (2010/63/EU) and from the Italian D.Leg 26/2014. and approved by the Italian Ministry of Health (Authorization No. 78/2017-PR).

For the *in vivo* toxicity assessment, all animal procedures were approved by the Institutional Animal Care and Use Committee of China Pharmaceutical University and performed in accordance with the established guidelines and policies for such evaluations (Approval No. YSL-202504091).

Data availability

All data supporting the findings of this study are included in the article and the supplementary information (SI). Supplementary figures, materials and methods are included in the SI file. See DOI: <https://doi.org/10.1039/d5nr03017j>.

Acknowledgements

This work was funded by the EU Horizon Europe Research and Innovation program Cancer Mission “HIT-GLIO” (2023-2027) (No. 101136835), the French National Research Agency under the framework of the Era-Net EURONANOMED European Research projects “iNanoGUN”, “NANOGLIO”, “TABRAINFECC” and “antineuropatho”, the National Key Research & Development Program of China for International S&T Cooperation Projects (2018YFE0117800), the Project Program of State Key Laboratory of Natural Medicines (China Pharmaceutical University, No. SKLNMZZ2024JS18), the Ligue Nationale Contre le Cancer (EL2016 and EL2021 LNCCLIP), and the China Scholarship Council (ZB: 202107067004 and WZ: 201906050186). SG was supported by “NextGenerationEU” (DD.3175/2021 E and DD. 3138/2021 CN_3) and the National Center for Gene Therapy and Drugs based on RNA Technology (CN 00000041); RF (GR-2021-12372494; PRIN 2022 2022488T5S). CL was supported by AIRC (IG2019 23010); MUR: “Progetto ECS 0000024 Rome Technopole, – CUP B83C22002820006, PNRR Missione 4 Componente 2 Investimento 1.5, finanziato dall’Unione europea – NextGenerationEU”. EL and SP acknowledge access to supercomputing resources and financial support from ICSC-Centro Nazionale di Ricerca in high-performance computing, big data, and quantum computing (Spoke 7: WP4 (Pilot applications), T.2.8 (Development and optimization of HPC-based integrated workflows based on flagship codes for personalized (nano)medicine); WP5 (Materials Foundry), T.2.3 (Development of computational workflows based on atomistic



molecular simulations for the prediction of key properties of molecular system and high-performance (nano)materials for biological, pharmaceutical and industrial application)).

References

- 1 E. Nance, S. H. Pun, R. Saigal and D. L. Sellers, Drug Delivery to the Central Nervous System, *Nat. Rev. Mater.*, 2021, **7**(4), 314–331, DOI: [10.1038/s41578-021-00394-w](https://doi.org/10.1038/s41578-021-00394-w).
- 2 W. Zhang, D. Xiao, Q. Mao and H. Xia, Role of Neuroinflammation in Neurodegeneration Development, *Signal Transduction Targeted Ther.*, 2023, **8**(1), 267, DOI: [10.1038/s41392-023-01486-5](https://doi.org/10.1038/s41392-023-01486-5).
- 3 A. N. Brandebura, A. Paumier, T. S. Onur and N. J. Allen, Astrocyte Contribution to Dysfunction, Risk and Progression in Neurodegenerative Disorders, *Nat. Rev. Neurosci.*, 2023, **24**(1), 23–39, DOI: [10.1038/s41583-022-00641-1](https://doi.org/10.1038/s41583-022-00641-1).
- 4 M. Colonna and O. Butovsky, Microglia Function in the Central Nervous System During Health and Neurodegeneration, *Annu. Rev. Immunol.*, 2017, **35**(1), 441–468, DOI: [10.1146/annurev-immunol-051116-052358](https://doi.org/10.1146/annurev-immunol-051116-052358).
- 5 D. Wu, Q. Chen, X. Chen, F. Han, Z. Chen and Y. Wang, The Blood–Brain Barrier: Structure, Regulation and Drug Delivery, *Signal Transduction Targeted Ther.*, 2023, **8**(1), 217, DOI: [10.1038/s41392-023-01481-w](https://doi.org/10.1038/s41392-023-01481-w).
- 6 R. Pandit, L. Chen and J. Götz, The Blood-Brain Barrier: Physiology and Strategies for Drug Delivery, *Adv. Drug Delivery Rev.*, 2020, **165–166**, 1–14, DOI: [10.1016/j.addr.2019.11.009](https://doi.org/10.1016/j.addr.2019.11.009).
- 7 A. Verkhratsky, A. Butt, B. Li, P. Illes, R. Zorec, A. Semyanov, Y. Tang and M. V. Sofroniew, Astrocytes in Human Central Nervous System Diseases: A Frontier for New Therapies, *Signal Transduction Targeted Ther.*, 2023, **8**(1), 396, DOI: [10.1038/s41392-023-01628-9](https://doi.org/10.1038/s41392-023-01628-9).
- 8 C. Gao, J. Jiang, Y. Tan and S. Chen, Microglia in Neurodegenerative Diseases: Mechanism and Potential Therapeutic Targets, *Signal Transduction Targeted Ther.*, 2023, **8**(1), 359, DOI: [10.1038/s41392-023-01588-0](https://doi.org/10.1038/s41392-023-01588-0).
- 9 W. Bi, T. Lei, S. Cai, X. Zhang, Y. Yang, Z. Xiao, L. Wang and H. Du, Potential of Astrocytes in Targeting Therapy for Alzheimer's Disease, *Int. Immunopharmacol.*, 2022, **113**, 109368, DOI: [10.1016/j.intimp.2022.109368](https://doi.org/10.1016/j.intimp.2022.109368).
- 10 A. Nakano-Kobayashi, A. Canela, T. Yoshihara and M. Hagiwara, Astrocyte-Targeting Therapy Rescues Cognitive Impairment Caused by Neuroinflammation via the Nrf2 Pathway, *Proc. Natl. Acad. Sci. U. S. A.*, 2023, **120**(33), e2303809120, DOI: [10.1073/pnas.2303809120](https://doi.org/10.1073/pnas.2303809120).
- 11 H. Liu, Y. Han, T. Wang, H. Zhang, Q. Xu, J. Yuan and Z. Li, Targeting Microglia for Therapy of Parkinson's Disease by Using Biomimetic Ultrasmall Nanoparticles, *J. Am. Chem. Soc.*, 2020, **142**(52), 21730–21742, DOI: [10.1021/jacs.0c09390](https://doi.org/10.1021/jacs.0c09390).
- 12 A. Lofts, F. Abu-Hijleh, N. Rigg, R. K. Mishra and T. Hoare, Using the Intranasal Route to Administer Drugs to Treat Neurological and Psychiatric Illnesses: Rationale, Successes, and Future Needs, *CNS Drugs*, 2022, **36**(7), 739–770, DOI: [10.1007/s40263-022-00930-4](https://doi.org/10.1007/s40263-022-00930-4).
- 13 D. Xu, X.-J. Song, X. Chen, J.-W. Wang and Y.-L. Cui, Advances and Future Perspectives of Intranasal Drug Delivery: A Scientometric Review, *J. Controlled Release*, 2024, **367**, 366–384, DOI: [10.1016/j.jconrel.2024.01.053](https://doi.org/10.1016/j.jconrel.2024.01.053).
- 14 Y. Chen, C. Zhang, Y. Huang, Y. Ma, Q. Song, H. Chen, G. Jiang and X. Gao, Intranasal Drug Delivery: The Interaction between Nanoparticles and the Nose-to-Brain Pathway, *Adv. Drug Delivery Rev.*, 2024, **207**, 115196, DOI: [10.1016/j.addr.2024.115196](https://doi.org/10.1016/j.addr.2024.115196).
- 15 L. Tang, R. Zhang, Y. Wang, M. Liu, D. Hu, Y. Wang and L. Yang, Nanoparticle Delivery for Central Nervous System Diseases and Its Clinical Application, *Nano Res.*, 2024, **17**(7), 6305–6322, DOI: [10.1007/s12274-024-6598-1](https://doi.org/10.1007/s12274-024-6598-1).
- 16 N. Rabiee, S. Ahmadi, R. Afshari, S. Khalaji, M. Rabiee, M. Bagherzadeh, Y. Fatahi, R. Dinarvand, M. Tahriri, L. Tayebi, M. R. Hamblin and T. J. Webster, Polymeric Nanoparticles for Nasal Drug Delivery to the Brain: Relevance to Alzheimer's Disease, *Adv. Ther.*, 2021, **4**(3), 2000076, DOI: [10.1002/adtp.202000076](https://doi.org/10.1002/adtp.202000076).
- 17 N. Kamei, K. Ikeda, Y. Ohmoto, S. Fujisaki, R. Shirata, M. Maki, M. Miyata, Y. Miyauchi, N. Nishiyama, M. Yamada, Y. Ohigashi and M. Takeda-Morishita, Insulin-Inspired Hippocampal Neuron-Targeting Technology for Protein Drug Delivery, *Proc. Natl. Acad. Sci. U. S. A.*, 2024, **121**(41), e2407936121, DOI: [10.1073/pnas.2407936121](https://doi.org/10.1073/pnas.2407936121).
- 18 K. Veys, Z. Fan, M. Ghobrial, A. Bouché, M. García-Caballero, K. Vriens, N. V. Conchinha, A. Seuwen, F. Schlegel, T. Gorski, M. Crabbé, P. Gilardoni, R. Ardicoglu, J. Schaffenrath, C. Casteels, G. De Smet, I. Smolders, K. Van Laere, E. D. Abel, S.-M. Fendt, A. Schroeter, J. Kalucka, A. R. Cantelmo, T. Wälchli, A. Keller, P. Carmeliet and K. De Bock, Role of the GLUT1 Glucose Transporter in Postnatal CNS Angiogenesis and Blood-Brain Barrier Integrity, *Circ. Res.*, 2020, **127**(4), 466–482, DOI: [10.1161/CIRCRESAHA.119.316463](https://doi.org/10.1161/CIRCRESAHA.119.316463).
- 19 Y. Anraku, H. Kuwahara, Y. Fukusato, A. Mizoguchi, T. Ishii, K. Nitta, Y. Matsumoto, K. Toh, K. Miyata, S. Uchida, K. Nishina, K. Osada, K. Itaka, N. Nishiyama, H. Mizusawa, T. Yamasoba, T. Yokota and K. Kataoka, Glycaemic Control Boosts Glucosylated Nanocarrier Crossing the BBB into the Brain, *Nat. Commun.*, 2017, **8**(1), 1001, DOI: [10.1038/s41467-017-00952-3](https://doi.org/10.1038/s41467-017-00952-3).
- 20 A. Badr, K. P. Daily, M. Eltobgy, S. Estfanous, M. H. Tan, J. C-T Kuo, O. Whitham, C. Carafice, G. Gupta, H. M. Amer, M. M. Shamseldin, A. Yousif, N. P. Deems, J. Fitzgerald, P. Yan, A. Webb, X. Zhang, M. Pietrzak, H. E. Ghoneim, P. Dubey, R. M. Barrientos, R. J. Lee, O. N. Kokiko-Cochran and A. O. Amer, Microglia-Targeted Inhibition of miR-17 via Mannose-Coated Lipid Nanoparticles Improves Pathology and Behavior in a Mouse Model of Alzheimer's Disease, *Brain, Behav., Immun.*, 2024, **119**, 919–944, DOI: [10.1016/j.bbi.2024.05.006](https://doi.org/10.1016/j.bbi.2024.05.006).
- 21 A. Sharma, J. E. Porterfield, E. Smith, R. Sharma, S. Kannan and R. M. Kannan, Effect of Mannose Targeting



- of Hydroxyl PAMAM Dendrimers on Cellular and Organ Biodistribution in a Neonatal Brain Injury Model, *J. Controlled Release*, 2018, **283**, 175–189, DOI: [10.1016/j.jconrel.2018.06.003](https://doi.org/10.1016/j.jconrel.2018.06.003).
- 22 Z. Lyu and L. Peng, Potent Drugless Dendrimers, *Nat. Biomed. Eng.*, 2017, **1**(9), 686–688, DOI: [10.1038/s41551-017-0136-3](https://doi.org/10.1038/s41551-017-0136-3).
- 23 R. M. Kannan, E. Nance, S. Kannan and D. A. Tomalia, Emerging Concepts in Dendrimer-based Nanomedicine: From Design Principles to Clinical Applications, *J. Intern. Med.*, 2014, **276**(6), 579–617, DOI: [10.1111/joim.12280](https://doi.org/10.1111/joim.12280).
- 24 P. Moscariello, D. Y. W. Ng, M. Jansen, T. Weil, H. J. Luhmann and J. Hedrich, Brain Delivery of Multifunctional Dendrimer Protein Bioconjugates, *Adv. Sci.*, 2018, **5**(5), 1700897, DOI: [10.1002/advs.201700897](https://doi.org/10.1002/advs.201700897).
- 25 Z. Lyu, L. Ding, A. Tintaru and L. Peng, Self-Assembling Supramolecular Dendrimers for Biomedical Applications: Lessons Learned from Poly(Amidoamine) Dendrimers, *Acc. Chem. Res.*, 2020, **53**(12), 2936–2949, DOI: [10.1021/acs.accounts.0c00589](https://doi.org/10.1021/acs.accounts.0c00589).
- 26 J. Chen, D. Zhu, X. Liu and L. Peng, Amphiphilic Dendrimer Vectors for RNA Delivery: State-of-the-Art and Future Perspective, *Acc. Mater. Res.*, 2022, **3**(5), 484–497, DOI: [10.1021/accountsmr.1c00272](https://doi.org/10.1021/accountsmr.1c00272).
- 27 V. Percec, D. A. Wilson, P. Leowanawat, C. J. Wilson, A. D. Hughes, M. S. Kaucher, D. A. Hammer, D. H. Levine, A. J. Kim, F. S. Bates, K. P. Davis, T. P. Lodge, M. L. Klein, R. H. DeVane, E. Aqad, B. M. Rosen, A. O. Argintaru, M. J. Sienkowska, K. Rissanen, S. Nummelin and J. Ropponen, Self-Assembly of Janus Dendrimers into Uniform Dendrimersomes and Other Complex Architectures, *Science*, 2010, **328**(5981), 1009–1014, DOI: [10.1126/science.1185547](https://doi.org/10.1126/science.1185547).
- 28 X. Liu, D. Dhumal, P. Santofimia-Castaño, J. Liu, M. Casanova, A. C. Garcia-Muñoz, T.-A. Perles-Barbacaru, A. Elkihel, W. Zhang, T. Roussel, C. Galanakou, J. Wu, E. Zerva, N. Dusetti, Y. Xia, X.-J. Liang, A. Viola, J. L. Iovanna and L. Peng, Self-Assembling Dendrimer Nanodrug Formulations for Decreased hERG-Related Toxicity and Enhanced Therapeutic Efficacy, *Sci. Adv.*, 2025, **11**(26), eadu9948, DOI: [10.1126/sciadv.adu9948](https://doi.org/10.1126/sciadv.adu9948).
- 29 Y. Jiang, Z. Lyu, B. Ralahy, J. Liu, T. Roussel, L. Ding, J. Tang, A. Kosta, S. Giorgio, R. Tomasini, X.-J. Liang, N. Dusetti, J. Iovanna and L. Peng, Dendrimer Nanosystems for Adaptive Tumor-Assisted Drug Delivery via Extracellular Vesicle Hijacking, *Proc. Natl. Acad. Sci. U. S. A.*, 2023, **120**(7), e2215308120, DOI: [10.1073/pnas.2215308120](https://doi.org/10.1073/pnas.2215308120).
- 30 T. Wei, C. Chen, J. Liu, C. Liu, P. Posocco, X. Liu, Q. Cheng, S. Huo, Z. Liang, M. Fermeglia, S. Pricl, X.-J. Liang, P. Rocchi and L. Peng, Anticancer Drug Nanomicelles Formed by Self-Assembling Amphiphilic Dendrimer to Combat Cancer Drug Resistance, *Proc. Natl. Acad. Sci. U. S. A.*, 2015, **112**(10), 2978–2983, DOI: [10.1073/pnas.1418494112](https://doi.org/10.1073/pnas.1418494112).
- 31 J. Chen, D. Zhu, B. Lian, K. Shi, P. Chen, Y. Li, W. Lin, L. Ding, Q. Long, Y. Wang, E. Laurini, W. Lan, Y. Li, A. Tintaru, C. Ju, C. Zhang, S. Pricl, J. Iovanna, X. Liu and L. Peng, Cargo-Selective and Adaptive Delivery of Nucleic Acid Therapeutics by Bola-Amphiphilic Dendrimers, *Proc. Natl. Acad. Sci. U. S. A.*, 2023, **120**(21), e2220787120, DOI: [10.1073/pnas.2220787120](https://doi.org/10.1073/pnas.2220787120).
- 32 J. Chen, A. Ellert-Miklaszewska, S. Garofalo, A. K. Dey, J. Tang, Y. Jiang, F. Clément, P. N. Marche, X. Liu, B. Kaminska, A. Santoni, C. Limatola, J. J. Rossi, J. Zhou and L. Peng, Synthesis and Use of an Amphiphilic Dendrimer for siRNA Delivery into Primary Immune Cells, *Nat. Protoc.*, 2021, **16**(1), 327–351, DOI: [10.1038/s41596-020-00418-9](https://doi.org/10.1038/s41596-020-00418-9).
- 33 Z. Lyu, B. Ralahy, T.-A. Perles-Barbacaru, L. Ding, Y. Jiang, B. Lian, T. Roussel, X. Liu, C. Galanakou, E. Laurini, A. Tintaru, S. Giorgio, S. Pricl, X. Liu, M. Bernard, J. Iovanna, A. Viola and L. Peng, Self-Assembling Dendrimer Nanosystems for Specific Fluorine Magnetic Resonance Imaging and Effective Theranostic Treatment of Tumors, *Proc. Natl. Acad. Sci. U. S. A.*, 2024, **121**(25), e322403121, DOI: [10.1073/pnas.2322403121](https://doi.org/10.1073/pnas.2322403121).
- 34 L. Ding, Z. Lyu, T. Perles-Barbacaru, A. Y. Huang, B. Lian, Y. Jiang, T. Roussel, C. Galanakou, S. Giorgio, C. Kao, X. Liu, J. Iovanna, M. Bernard, A. Viola and L. Peng, Modular Self-Assembling Dendrimer Nanosystems for Magnetic Resonance and Multimodality Imaging of Tumors, *Adv. Mater.*, 2024, **36**(7), 2308262, DOI: [10.1002/adma.202308262](https://doi.org/10.1002/adma.202308262).
- 35 P. Garrigue, J. Tang, L. Ding, A. Bouhleb, A. Tintaru, E. Laurini, Y. Huang, Z. Lyu, M. Zhang, S. Fernandez, L. Balasse, W. Lan, E. Mas, D. Marson, Y. Weng, X. Liu, S. Giorgio, J. Iovanna, S. Pricl, B. Guillet and L. Peng, Self-Assembling Supramolecular Dendrimer Nanosystem for PET Imaging of Tumors, *Proc. Natl. Acad. Sci. U. S. A.*, 2018, **115**(45), 11454–11459, DOI: [10.1073/pnas.1812938115](https://doi.org/10.1073/pnas.1812938115).
- 36 Z. Shi, M. Artemenko, W. Yu, M. Zhang, C. Yi, P. Chen, S. Lin, Z. Bian, B. Lian, F. Meng, J. Chen, T. Roussel, Y. Li, K. K. L. Chan, P. P. C. Ip, H.-C. Lai, S. K. Y. To, X. Liu, L. Peng and A. S. T. Wong, Bola-Amphiphilic Dendrimer Enhances Imatinib to Target Metastatic Ovarian Cancer via β -Catenin-HRP2 Signaling Axis, *ACS Appl. Mater. Interfaces*, 2025, **17**(2), 2884–2898, DOI: [10.1021/acsami.4c12857](https://doi.org/10.1021/acsami.4c12857).
- 37 X. Liu, Y. Wang, C. Chen, A. Tintaru, Y. Cao, J. Liu, F. Ziarelli, J. Tang, H. Guo, R. Rosas, S. Giorgio, L. Charles, P. Rocchi and L. Peng, A Fluorinated Bola-Amphiphilic Dendrimer for On-Demand Delivery of siRNA, via Specific Response to Reactive Oxygen Species, *Adv. Funct. Mater.*, 2016, **26**(47), 8594–8603, DOI: [10.1002/adfm.201604192](https://doi.org/10.1002/adfm.201604192).
- 38 H. Zeng, M. E. Johnson, N. J. Oldenhuis, T. N. Tiambeng and Z. Guan, Structure-Based Design of Dendritic Peptide Bolaamphiphiles for siRNA Delivery, *ACS Cent. Sci.*, 2015, **1**(6), 303–312, DOI: [10.1021/acscentsci.5b00233](https://doi.org/10.1021/acscentsci.5b00233).
- 39 D. L. Valentine, Adaptations to Energy Stress Dictate the Ecology and Evolution of the Archaea, *Nat. Rev. Microbiol.*, 2007, **5**(4), 316–323, DOI: [10.1038/nrmicro1619](https://doi.org/10.1038/nrmicro1619).
- 40 W. Zhang, D. Dhumal, X. Zhu, B. Ralahy, A. Ellert-Miklaszewska, J. Wu, E. Laurini, Y. Yao, C. Kao, J. L. Iovanna, S. Pricl, B. Kaminska, Y. Xia and L. Peng,



- Bola-Amphiphilic Glycodendrimers: New Carbohydrate-Mimicking Scaffolds to Target Carbohydrate-Binding Proteins, *Chem. – Eur. J.*, 2022, **28**(58), e202201400, DOI: [10.1002/chem.202201400](https://doi.org/10.1002/chem.202201400).
- 41 J. J. Lundquist and E. J. Toone, The Cluster Glycoside Effect, *Chem. Rev.*, 2002, **102**(2), 555–578, DOI: [10.1021/cr000418f](https://doi.org/10.1021/cr000418f).
- 42 L. Su, Y. Feng, K. Wei, X. Xu, R. Liu and G. Chen, Carbohydrate-Based Macromolecular Biomaterials, *Chem. Rev.*, 2021, **121**(18), 10950–11029, DOI: [10.1021/acs.chemrev.0c01338](https://doi.org/10.1021/acs.chemrev.0c01338).
- 43 A. C. Rodrigo, S. M. Bromfield, E. Laurini, P. Posocco, S. Pricl and D. K. Smith, Morphological Control of Self-Assembled Multivalent (SAMul) Heparin Binding in Highly Competitive Media, *Chem. Commun.*, 2017, **53**(47), 6335–6338, DOI: [10.1039/C7CC02990J](https://doi.org/10.1039/C7CC02990J).
- 44 P. Garrigue, J. Tang, L. Ding, A. Bouhrel, A. Tintaru, E. Laurini, Y. Huang, Z. Lyu, M. Zhang, S. Fernandez, L. Balasse, W. Lan, E. Mas, D. Marson, Y. Weng, X. Liu, S. Giorgio, J. Iovanna, S. Pricl, B. Guillet and L. Peng, Self-Assembling Supramolecular Dendrimer Nanosystem for PET Imaging of Tumors, *Proc. Natl. Acad. Sci. U. S. A.*, 2018, **115**(45), 11454–11459, DOI: [10.1073/pnas.1812938115](https://doi.org/10.1073/pnas.1812938115).
- 45 L. Ding, Z. Lyu, B. Louis, A. Tintaru, E. Laurini, D. Marson, M. Zhang, W. Shao, Y. Jiang, A. Bouhrel, L. Balasse, P. Garrigue, E. Mas, S. Giorgio, J. Iovanna, Y. Huang, S. Pricl, B. Guillet and L. Peng, Surface Charge of Supramolecular Nanosystems for In Vivo Biodistribution: A MicroSPECT/CT Imaging Study, *Small*, 2020, **16**(37), 2003290, DOI: [10.1002/sml.202003290](https://doi.org/10.1002/sml.202003290).
- 46 M. Cong, G. Xu, S. Yang, J. Zhang, W. Zhang, D. Dhumal, E. Laurini, K. Zhang, Y. Xia, S. Pricl, L. Peng and W. Zhao, A Self-Assembling Prodrug Nanosystem to Enhance Metabolic Stability and Anticancer Activity of Gemcitabine, *Chin. Chem. Lett.*, 2022, **33**(5), 2481–2485, DOI: [10.1016/j.cclet.2021.11.083](https://doi.org/10.1016/j.cclet.2021.11.083).
- 47 T. R. Hammond, C. Dufort, L. Dissing-Olesen, S. Giera, A. Young, A. Wysoker, A. J. Walker, F. Gergits, M. Segel, J. Nimesh, S. E. Marsh, A. Saunders, E. Macosko, F. Ginhoux, J. Chen, R. J. M. Franklin, X. Piao, S. A. McCarroll and B. Stevens, Single-Cell RNA Sequencing of Microglia throughout the Mouse Lifespan and in the Injured Brain Reveals Complex Cell-State Changes, *Immunity*, 2019, **50**(1), 253–271, DOI: [10.1016/j.immuni.2018.11.004](https://doi.org/10.1016/j.immuni.2018.11.004).
- 48 Q. Li, Z. Cheng, L. Zhou, S. Darmanis, N. F. Neff, J. Okamoto, G. Gulati, M. L. Bennett, L. O. Sun, L. E. Clarke, J. Marschallinger, G. Yu, S. R. Quake, T. Wyss-Coray and B. A. Barres, Developmental Heterogeneity of Microglia and Brain Myeloid Cells Revealed by Deep Single-Cell RNA Sequencing, *Neuron*, 2019, **101**(2), 207–223, DOI: [10.1016/j.neuron.2018.12.006](https://doi.org/10.1016/j.neuron.2018.12.006).

